

Exploiting the Full Potential of the Advanced Two-hexapole Corrector for STEM

Ryusuke Sagawa^{1*}, Akira Yasuhara¹, Hiroki Hashiguchi¹, Tomoyuki Naganuma¹, Shinichi Tanba¹, Takaki Ishikawa¹, Thomas Riedel², Peter Hartel², Martin Linck², Stephan Uhlemann², Heiko Müller², and Hidetaka Sawada³

¹JEOL Ltd., 3-1-2 Musashino, Akishima, Tokyo, Japan

²Corrected Electron Optical Systems GmbH, Englerstr. 28, Heidelberg, Germany

³JEOL USA, Inc., 11 Dearborn Road Peabody, MA, USA

*Corresponding author: rsagawa@jeol.co.jp

During the last decades the achievable spatial resolution as well as the usable aperture angle of the scanning transmission electron microscope (STEM) improved tremendously. The first big step owes to the correction of the third-order spherical aberration C_3 of the objective lens e.g. by means of a two-hexapole design (CESCOR) [1]. In a next step the inevitable fifth-order six-fold astigmatism A_5 of two-hexapole correctors was almost eliminated by optimizing the geometry of the hexapoles and the transfer lenses (DCOR/ASCOR) [2]. The usage of larger aperture angles, however, demands an accurate planning of high-resolution experiments including a careful review of the effect of the sixth- and higher-order axial aberrations. In addition, an optimum aperture semi-angle and maximum usable probe current have to be considered. In this work, we theoretically derived optimum parameters and successfully achieved higher resolution in STEM.

Firstly, an optimum aperture semi-angle α with respect to diffraction limit and the effect of the chromatic aberration has to be determined. For our experimental setup at 60 kV, it was determined to be 37.4 mrad using eq. (4) in [3]. Next, the state of the aberrations has to be optimized for this aperture semi-angle. In principle higher-order aberrations can partly be compensated by lower-order aberrations of the same multiplicity [4]. For the state-of-the-art two-hexapole corrector, the first relevant intrinsic aberration is the non-vanishing sixth-order three-lobe aberration D_6 which can be compensated by fourth-order three-lobe aberration D_4 . The size of the intrinsic D_6 is defined by geometrical and optical properties of the corrector and the pole piece at the chosen high tension. For our experimental conditions, the theoretical prediction for the intrinsic aberrations A_5 and D_6 amounts to $A_{5y} = 0.17$ mm and $D_{6x} = +4$ mm, respectively, with vanishing A_{5x} and negligible D_{6y} [3,5]. Fig. 1 shows simulated electron probe phase maps with various D_4 values at 60 kV. Without any compensation of D_6 with D_4 , i.e. when D_{4x} is 0.0 μm , the phase looks relatively flat but the simulated electron probe has a faint three-fold side lobe (Fig. 1(a)). With a mistuned D_{4x} of -23 μm , the phase has a smaller flat area and the probe has a strong three-fold structure (Fig. 1(b)). One has to be careful that although the flat area in Ronchigram image in this condition looks larger, the actual electron phase is not optimized at all. Fig. 1(c) shows a phase map with optimum compensation with D_{4x} of -4.8 μm . Up to the aperture semi-angle, the phase is significantly flatter than that in (a) and (b), and the probe has an almost perfectly round shape.

With the optimized corrector condition, we recorded high-resolution STEM images using a JEOL CFEG NEOARM microscope equipped with a CEOS ASCOR corrector operated at 60 kV. We chose an aperture semi-angle of 38 mrad and an energy spread of 0.34 eV since the condition should give the optimum probe shape for 60 kV [3]. The probe current was set to 16 pA. Fig. 2 shows an ADF-STEM image of a Si[112] sample recorded under that condition. In the FFT pattern (Fig. 2(b)), the spots corresponding to the 73 pm spacings ((2 6 4) reflections) are visible, which was confirmed to be

consistent with the result of a multi-slice image simulation. Since the negligible residual A_5 has no influence on STEM resolution, we could achieve higher resolution without adding additional optical elements such as A_5 stigmators.

References:

- [1] M Haider *et al.*, *Ultramicroscopy*, **81** (2000) p. 163.
- [2] H Müller *et al.*, *Microscopy and Microanalysis*, **12** (6) (2008) p. 442.
- [3] R Sagawa *et al.*, *Ultramicroscopy*, **233** (2022) p. 113440.
- [4] S Morishita *et al.*, *Physical Review Letters*, **117** (15) (2016) p. 153004.
- [5] P Hartel *et al.*, *Ultramicroscopy*, **206** (2019) p. 112821.

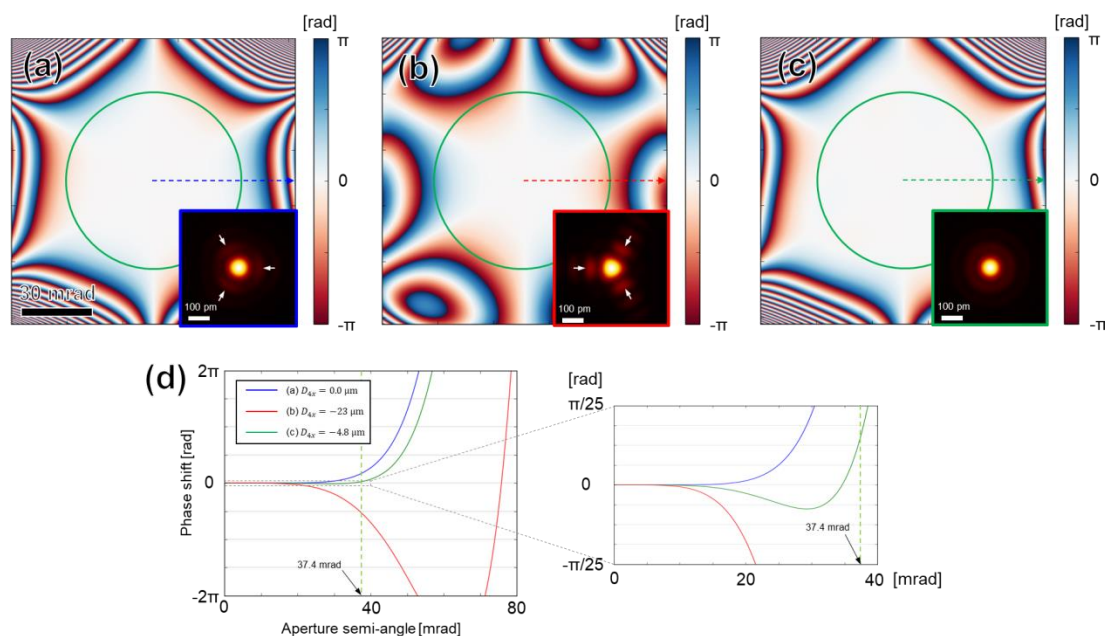


Figure 1. Simulated probe phase maps and electron probes in insets with a 37.4 mrad aperture semi-angle (green circles). (a) Without D_4 compensation. D_{4x} is 0.0 μm . (b) With a mistuned D_4 . D_{4x} is -23 μm . (c) With optimum D_4 compensation for the chosen aperture semi-angle of 37.4 mrad. D_{4x} is -4.8 μm . (d) Radial wave aberration plotted along the horizontal dashed lines in (a) to (c) (left) and magnified plot (right). The condition $D_{4x} = -4.8 \mu\text{m}$ (green plot) minimizes the phase shift up to 37.4 mrad.

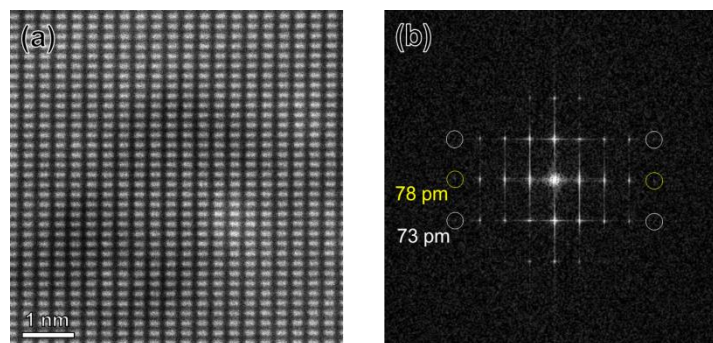


Figure 2. ADF-STEM images of a Si[112] sample recorded at 60 kV. (a) ADF-STEM image obtained by averaging 20 ADF-STEM images of 1024×1024 pixels with a dwell time of 2 $\mu\text{s}/\text{pixel}$ and (b) FFT pattern of (a). The spots corresponding to the 73 pm spacings are visible.